



Volume 253, No. 19, 31 July 2007 ISSN 0169-4332

applied surface science

A journal devoted to applied physics
and chemistry of surfaces and interfaces

Proceedings of the European Materials
Research Society 2006 - Symposium-H

Photon-Assisted Synthesis and Processing of Functional Materials
Nice, France - May 29-June 2, 2006

Organizers:

Maria Dinescu, Hiroshi Fukumura, Henry Helvajian,
Eric Millon, Tamas Szoranyi

Volume 253, No. 19, pp. 7645-8334

31 July 2007

Available online at www.sciencedirect.com

ScienceDirect
<http://www.elsevier.com/locate/apsusc>

This article was published in an Elsevier journal. The attached copy is furnished to the author for non-commercial research and education use, including for instruction at the author's institution, sharing with colleagues and providing to institution administration.

Other uses, including reproduction and distribution, or selling or licensing copies, or posting to personal, institutional or third party websites are prohibited.

In most cases authors are permitted to post their version of the article (e.g. in Word or Tex form) to their personal website or institutional repository. Authors requiring further information regarding Elsevier's archiving and manuscript policies are encouraged to visit:

<http://www.elsevier.com/copyright>

Micro-structuring of TiO₂ thin films by laser-assisted diffraction processing

O. Van Overschelde, G. Guisbiers, M. Wautelet*

Condensed Matter Physics Group, University of Mons-Hainaut, 23, B-7000 Mons, Belgium

Available online 25 February 2007

Abstract

Thin films of TiO₂ are deposited by magnetron sputtering on glass substrate and are irradiated by UV radiation using a KrF excimer laser (248 nm). These thin films are patterned with a razor blade placed on the way of the radiation just in front of the TiO₂ thin film. Just near the edge of the razor blade on the thin film, diffraction lines are observed, resulting in the ablation of the film. These patterns are characterized by optical microscopy, mechanical profilometry. Diffraction up to the 35th order is observed. The results are shown to be compatible with a model in which electronic excitation plays the major role.

© 2007 Elsevier B.V. All rights reserved.

Keywords: Titanium dioxide films; Laser processing; Thin films; Microstructuring; Diffraction

1. Introduction

There is currently a large number of works dealing with the scientific and technological properties of TiO₂ [1]. Titanium dioxide is used in applications as diverse as heterogeneous catalysis, photocatalysis, solar cells, gas sensors, white pigments, corrosion-protective coating, optical coating, ceramics, electric devices. It plays a role in earth science, biocompatibility. It is discussed as a component in microelectronics and in nanotechnology. There is also a need to better understand the physical and chemical properties of the two main crystallographic structures of TiO₂, namely rutile and anatase.

Since TiO₂ is expected to play a role in nano- and microtechnologies, it is interesting to study various methods of nano- or microstructuring it. Laser treatment is one of the main techniques for designing nano- and microstructures. The irradiation of TiO₂ by laser sources has been reported on powders, monocrystals [2–4]. This is shown to induce phase transitions as well as colour changes, due to surface reduction. We recently reported laser etching of TiO₂ [5].

Laser interactions with thin films may lead to various processes, like melting, ablation, texturing, hardening [6]. When laser irradiation is performed in air, plasmas may be

created at high fluence, giving rise to positive as well as negative feedbacks. Moreover, the processes may be either purely thermal, or photolytic. It is then necessary to perform careful experimental studies, in order to better understand the involved physico-chemical mechanisms.

One procedure is to study the effects of laser irradiations at various fluences, F . It is also possible to vary F locally by taking into account diffraction effects. It is the aim of this work to study the effects of diffraction-assisted irradiation on the structure of thin films.

2. Experimental details

TiO₂ films are deposited on glass by magnetron sputter deposition. The coating chamber is an industrial system (TSD 400-CD HEF R&D) with various diagnostic facilities such as optical emission and mass spectrometers. The area of the titanium target is 450 mm × 150 mm and its thickness 8 mm. The target is sputtered in dc mode with a ENIRPG 100 generator. The maximum power is 10 kW with a maximum voltage of 800 V. In the following, the experiments are performed on 208 nm thick TiO₂ films on glass (area: 7.5 cm × 24 cm).

The films are irradiated in air, by means of a Lambda Physik (Model Compex 205) excimer laser ($\lambda = 248$ nm). The pulse duration is given to be $\tau = 25$ ns. The laser fluence is changed by varying the distance between a UV lens ($f = 250$ mm), and the sample.

* Corresponding author. Tel.: +32 65373325.

E-mail address: michel.wautelet@umh.ac.be (M. Wautelet).

In order to produce non-uniform and well characterized spatially resolved laser irradiation, a razor blade is placed in contact with the films. The distance between the edge of the razor blade and the film is measured to be 55 μm. This experimental set-up gives rise to a border diffraction effect, hence a non-uniform but well known irradiation pattern. The irradiation fluence is varied between 100 and 1550 mJ/cm².

After irradiation, the thicknesses of the irradiated films are evaluated by means of a DEKTAK 3030ST profilometer.

3. Experimental results

Typical optical microscope images and the corresponding profilometry measurements of the irradiated films are given in Figs. 1 and 2, respectively. Four main regimes are observed. At low F (<100 mJ/cm²), no transformation takes place, as seen visually and measured by profilometry. Increasing F , at $F \sim 100$ mJ/cm², some transformation occurs, as seen visually. The structure follows the local laser fluence. Profilometry measurements indicate that the total thickness of the films increase by 10–100 nm above the starting level. When F increases further, a complex structure is observed. When F attains a value of 1250 mJ/cm², the regular structure appears, with ablation of the films. At very high F (>1550 mJ/cm²), films detach from the substrate. Altogether, it turns out that a regularly structured system appears in two narrow fluence regimes, between about 100 and 120 mJ/cm², and about 1250 and 1550 mJ/cm².

4. Discussion

Since the microscopy and profilometry measurements indicate oscillations in the structure of the laser-irradiated films, it is necessary to first evaluate the laser-diffracted fluence at the film level.

4.1. Diffraction

In the present experiments, diffraction by a border occurs. In this case, the intensity profile is given by the well-known

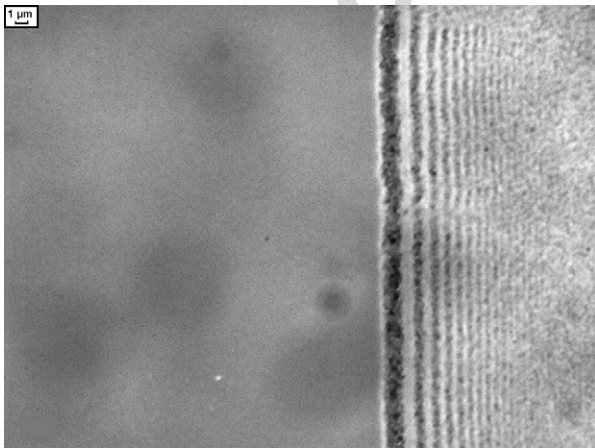


Fig. 1. Optical microscopy and profilometry of the laser irradiated film ($F = 120$ mJ/cm²).

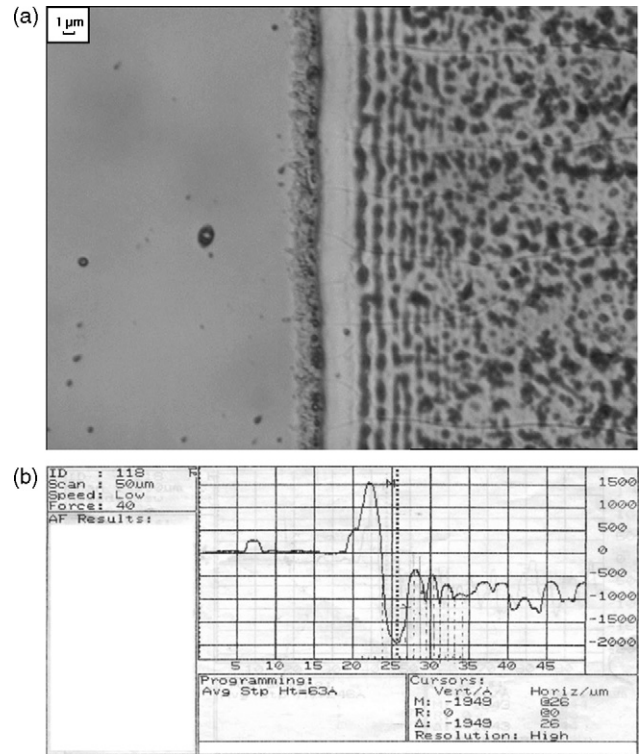


Fig. 2. Optical microscopy and profilometry of the laser irradiated film ($F = 1550$ mJ/cm²).

diffraction theory [7]. It is given by:

$$I = \frac{I_0}{2} \left\{ \left[\frac{1}{2} - C(v) \right]^2 + \left[\frac{1}{2} - S(v) \right]^2 \right\} \tag{1}$$

In this equation, I_0 is the incident fluence of the laser beam, $C(v)$ and $S(v)$ are the real and imaginary part of the complex Fresnel integral, respectively; v is the Fresnel parameter:

$$v = x \sqrt{\left(\frac{2}{D\lambda} \right)} \tag{2}$$

λ is the laser wavelength and D is the razor-sample distance. I is calculated and plotted by the Maple 9.5 software for all our experimental conditions.

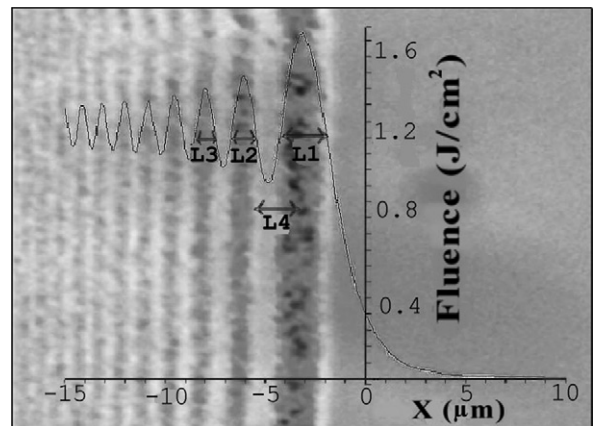


Fig. 3. Fitting of intensity profile vs. structure.

Table 1
Theoretical and observed structure characteristics (see Fig. 3)

	L1 Th. (μm) $\pm (0.05 \mu\text{m})$	L2 Th. (μm) $\pm (0.05 \mu\text{m})$	L3 Th. (μm) $\pm (0.05 \mu\text{m})$	L4 Th. (μm) $\pm (0.05 \mu\text{m})$	L1 Exp. (μm) $\pm (0.14 \mu\text{m})$	L2 Exp. (μm) $\pm (0.14 \mu\text{m})$	L2 Exp. (μm) $\pm (0.14 \mu\text{m})$	L4 Exp. (μm) $\pm (0.14 \mu\text{m})$
$F = 100 \text{ mJ/cm}^2$	2.16	1.23	0.82	1.69	2.00	1.14	0.86	2.29
$F = 120 \text{ mJ/cm}^2$	2.16	1.23	0.82	1.69	2.29	1.14	0.86	1.71
$F = 1250 \text{ mJ/cm}^2$	2.16	1.23	0.82	1.69	2.86	1.29	1.00	2.57
$F = 1550 \text{ mJ/cm}^2$	2.16	1.23	0.82	1.69	3.14	1.14	1.00	2.86

Table 2
Theoretical and observed ablated structure characteristics

	Theory Fraction of the maximum intensity variation (AB) for the gain of intensity between B and C (%)	Profilometry Fraction of the maximum height variation (AB) for the loss of height between B and C (%)
$F = 100 \text{ mJ/cm}^2$	10.4 ± 0.01	12.2 ± 1
$F = 120 \text{ mJ/cm}^2$	10.4 ± 0.01	11.5 ± 1
$F = 1550 \text{ mJ/cm}^2$	10.4 ± 0.01	9.5 ± 1

The diffraction pattern is compared with the experimental data, as shown in Fig. 3 and Table 1. It turns out that the structure of the irradiated films compare very well with the diffraction pattern up to the 4th order. This means that this procedure allows to design structures in the micron range. It is worth noting that, for $F = 100 \text{ mJ/cm}^2$, a structure is observed up to the 35th order where the line width is equal to 269 nm.

4.2. Low fluence laser-induced transformation

In the 100–120 mJ/cm^2 range, the laser-irradiated films are thicker than the original films (Fig. 1). A similar behaviour is observed in the same fluence range, in the case of uniform excimer-laser irradiation [5]. This is tentatively associated with the crystallization of the initially amorphous film. Although the lateral characteristics of the structure mimics the diffraction pattern, it is not yet possible to relate the thickness variations with the fluence oscillations.

4.3. Laser-induced ablation

In the 1250–1550 mJ/cm^2 range, the laser-irradiated films are seen to be ablated. In order to understand the origin of the ablation process, the ablated profile is fitted by the diffracted fluence oscillations functions. Results are summarized in Table 2. The fluence at the extrema of the diffraction pattern are compared with the height variations at the corresponding points of the films, as measured by profilometry. (Fig. 4 is displayed only for explanation of calculus.)

In order to understand the origin of this phenomena we would analyse how the variation of the height of the surface is in accord with the variations of the intensity. unfortunately, profilometry give us information about topography of the surface but only for the mount and not for the hole. So we work only for the first peak of intensity who corresponds to the first hole in the surface. The loss of intensity from the first peak and the first minima represent the maximum variation of intensity, this will be our reference for comparing the gain between B and C. We assume in the same manner by profilometry that the

variation of height between A and B is the maximum variation of height and we will compare the loss of height between B and C with this maximum height variation (see Table 2), the ratio between the theoretical fluence between points B and C and points A and B (see Fig. 4) are compared with the corresponding ratios of the profilometry. They are reported in Table 2. It turns out that the variations agree quantitatively.

We also measured the ablated thickness as a function of the local fluence. Results are given in Fig. 5. It turns out that, in this regime, the ablated depth varies linearly with the local fluence.

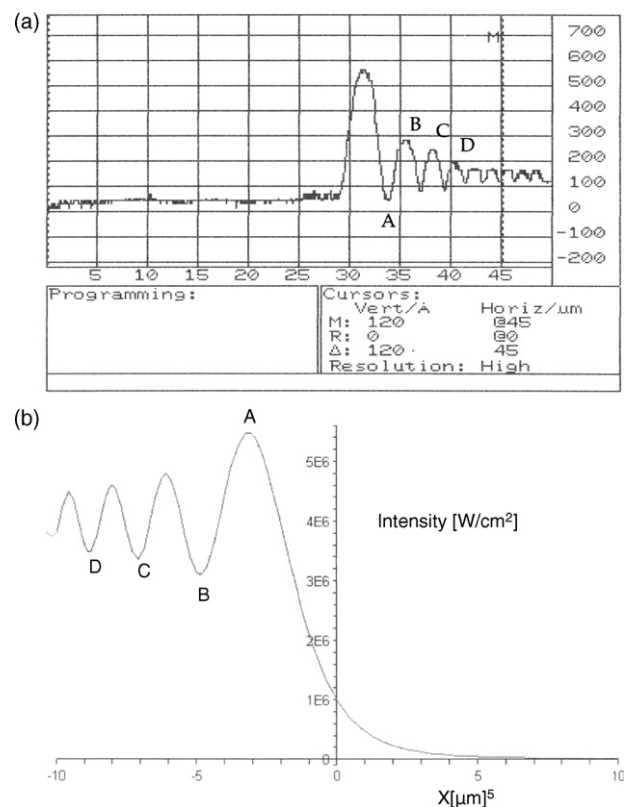


Fig. 4. Profilometry measurement ($F = 1250 \text{ mJ/cm}^2$) and theoretical diffraction fluence profile.

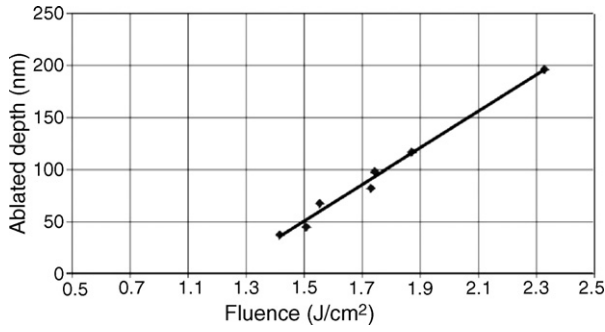


Fig. 5. Variation of the ablated depth at various local fluences.

In a previous work [5], it has been argued that the excimer-laser ablation of TiO₂ films may be explained either by a thermal model or by electronic effects or by a combination of both. Let us look at the possible mechanisms. The starting point of any laser-induced effect is the absorption of electromagnetic energy by the solid. Part of the electromagnetic energy is reflected by the surface. The initial reflectivity, R , is easily calculated via the knowledge of the complex refractive index of the film at the irradiating wavelength [8]. In our case, $R = 0.27$. The non-reflected energy is absorbed within a thin layer, characterized by the optical absorption depth, δ , obtained from the optical constants of the film. Here, $\delta = 15$ nm. Since the thickness of the films is higher (208 nm) than δ , the energy is absorbed within the film.

The absorption of light occurs by excitation of electrons from occupied to unoccupied energy states. When the photon energy, $h\nu$, is larger than the fundamental bandgap, E_g , the main absorption paths couple delocalized states. When $h\nu < E_g$, optical absorption involves either localized states (associated with defects, impurities or the surface) or delocalized surface states. In our case, $h\nu = 5$ eV $> E_g \approx 3$ eV.

The optically excited states are obviously unstable. The system decays by a combination (spatial and temporal) of various processes involving electrons, phonons and atoms (or vacancies). This results in heating of the lattice. When both the light absorption depth, δ , and the mean free path of the electrons are much less than the dimensions of the irradiated sample, laser heating may be viewed as localized at the irradiated surface. The equations governing the depth dependent temperature, T , are now well known. When heating is sufficient, phase transitions (melting, vaporization) may occur. The energy absorbed in the irradiated zone serves to heat it, the substrate and the surrounding atmosphere. Under our experimental conditions, it is well established that absorption within the plasma plume is negligible [6].

A correct evaluation of the energy effectively provided to transform the sample requires careful calculations of the role of the sample itself. When dealing with processes such as vaporization, it is also necessary to take into account the fact that it is a non-isothermal one, with a strong Arrhenius-type temperature dependence of the evaporation rate constant, R .

However, it may be argued that the present results are not explained by a purely thermal model. Indeed, the linear dependence of the ablated thickness with F is observed when F

varies by a factor of .5. If the mechanism is dictated by an Arrhenius laws, it would not be vary linearly over such a range.

Let us now examine the possible role of electronic effects. It is known that TiO₂ is a photocatalyst. This means that photoexcited electrons play a role in surface reactions. There are different mechanisms relevant to surface effects. One of them is the breaking of surface chemical bonds, responsible for evaporation. In the framework of the modeling of photo-assisted surface effects, it has been argued [9] that the cohesive properties of electronically excited states are different from the ones of non-excited ones. In the case of covalent bonds, the activation energy for bond breaking is expressed by [9]:

$$E_b = H_b - TS_b \quad (3a)$$

$$H_b = M + U(1 - cn) \quad (3b)$$

S is the associated entropy. M is a so-called metallic part. U is related to the strength of the covalent bond. n is the electron density associated with one excited covalent bond. n^{-1} is the number of atoms among which the electronic excitation is shared. In other words, it is a measure of the spatial extension of the wavefunction of the excited state. Therefore, for the non-excited state, $E_b = E_b(n = 0) = M + U - TS_b(n = 0)$. It has been calculated that:

$$\Delta S_b = S_b(n) - S_b(0) = -\left(\frac{3}{2}\right)kn^{-1}\ln(1 - cn) > 0. \quad (4)$$

Since H_b and S_b both decrease with increasing n (hence by electronic excitation), E_b may either increase or decrease.

The overall desorption rate also depends on the number of electronically excited states. This is expected to be proportional to the instantaneous fraction of photoexcited electrons, f .

Altogether, the total evaporation rate, R_{tot} , is the sum of the non-excited, R_{ne} , and excited, R_e , contributions:

$$\begin{aligned} R_{tot} &= R_{ne} + R_e \\ &= R_0 \left[(1 - f) \exp\left(\frac{S_b(0)}{k}\right) \exp\left(\frac{-H_b(0)}{kT}\right) \right. \\ &\quad \left. + f \exp\left(\frac{S_b(n)}{k}\right) \exp\left(\frac{-H_b(n)}{kT}\right) \right] \\ &= R' + fR'' \end{aligned} \quad (5)$$

Let us assume that the photoexcited sites are characterized by a higher ablation rate than the non-excited ones, i.e. $R'' > R'$. In this case, the higher the number of excited electrons, the higher the ablation rate. Moreover, the ablation rate varies linearly with F , since F is proportional to f . This is in agreement with other authors arguing that excimer laser irradiation leads to photochemical ablation [10].

Altogether, the previous reasoning indicates that the experimental results may be explained by electronic effects. Theoretical and experimental works are in progress in order to verify this on other experimental conditions.

5. Conclusions

The present work shows that, under KrF excimer laser irradiation, sputter deposited TiO₂ thin films on glass may be ablated. At low fluence, nothing occurs. When the fluence increases, one observes a transformation of the system to a thicker and rougher film. This is tentatively associated with the crystallization of the initially amorphous film. We showed that it is possible to pattern a diffraction structure on TiO₂ thin film, that diffraction pattern could appear in the two regime observed in TiO₂ irradiation. There are two threshold observed, one for each regime and between this two ones no structure appear, the pattern is lost in the roughness of the surface. We proved that the induced structures match correctly with the intensity variations of the illumination field. We could conclude that micro-structuring by diffraction could be controlled by diffraction effects.

References

- [1] Y. Leprince-Wang, K. Yu-Zhang, *Surf. Coat. Technol.* 140 (2001) 155–160.
- [2] T. Le Mercier, J.-M. Mariot, P. Parent, M.-F. Fontaine, C.F. Hague, M. Quarton, *Appl. Surf. Sci.* 86 (1995) 382.
- [3] T.D. Robert, L.D. Laude, V.M. Geskin, R. Lazzaroni, R. Gouttebaron, *Thin Solid Films* 440 (2003) 268.
- [4] Y.-J. Li, T. Matsumoto, N. Gu, M. Komiyama, *Appl. Surf. Sci.* 237 (2004) 374.
- [5] O. Van Overschelde, S. Dinu, G. Guisbiers, F. Monteverde, C. Nouvellon, M. Wautelet, *Appl. Surf. Sci.*, in press.
- [6] D. Bauerle, *Laser Processing and Chemistry*, Springer, Berlin, 2000.
- [7] M. Born, E. Wolf, *Principles of Optics*, seventh ed., Cambridge University Press, Cambridge, 1999.
- [8] E.D. Palik (Ed.), *Handbook of Optical Constants of Solids*, Academic Press, Orlando, 1985.
- [9] M. Wautelet, E.D. Gehain, *Semicond. Sci. Technol.* 5 (1990) 246.
- [10] F. Brygo, Ch. Dutouquet, F. Le Guern, R. Oltra, A. Semerok, J.M. Weulersse, *Appl. Surf. Sci.* 252 (2006) 2131.